International Journal of Hydrogen Energy 105 (2025) 1435–1450

Contents lists available at ScienceDirect

International Journal of Hydrogen Energy

journal homepage: www.elsevier.com/locate/he

# Comparison of game theory and genetic algorithm optimisation schedulers for diesel-hydrogen powered system reconfiguration

Hadi Taghavifar [a,*], Sumit Roy [a,b], Anthony Paul Roskilly [a]

[a] Department of Engineering, Durham University, Durham, DH1 3LE, UK

[b] Centre for E-Mobility and Clean Growth, Coventry University, Coventry, CV1 2TL, UK

ARTICLE INFO

Handling Editor: M Djukic

*Keywords:*
*Hydrogen*
*Multiobjective game theory*
*NSGA-II*
Optimisation
Powertrain Modelling

ABSTRACT

The turbocharged dual-fuel engine is modeled and connected online to optimiser platform for transient input variation of input parameters decided by designed algorithms. This task is undertaken to enable intelligent control of the propulsion system including the Hydrogen injection instantly to reduce the thermal irreversibility. Therefore, two methods of optimisation are applied to data collected from a turbocharged dual fuel operated propulsion system with direct diesel fuel injection and hydrogen port injection. This study investigates the application of multi-objective game theory (MOGT) and non-dominated sorting genetic algorithm II (NSGA-II) for optimising the performance of a diesel-hydrogen dual-fuel engine. The system is designed in 1D framework with input variability of the turbocharger efficiency, hydrogen mass injection, air compression ratio (Rp), and start of combustion (SoC). The objective is to set maximized the volume work while minimising the entropy generation and NO emission. The first populations in the optimisation procedures are initialised with uniform Latin hypercube and random space filler design of experiment (DoE) for both optimisers. The MOGT can find the best solution faster than NSGA-II with slightly better result. The statistics showed that MOGT generates 12 more unfeasible designs that do not meet the constraint limit on NO emission. The findings indicate that for different optimisation algorithms there are some factors with different effect direction and size on the objectives. Additionally, it is discovered that although MOGT solution makes higher objective function value, the NSGA-II optimal solution leads to better engine efficiency and lower fuel consumption.

## 1. Introduction

The efforts for hydrogen engines are still on progress along with the research on hydrogen production, storage, and utilization. The reason for using hydrogen in the internal combustion engine (ICE) as alternative fuel is mainly to control the CO2 emissions and the ambition towards the decarbonization target. Clean and renewable hydrogen is beneficial to achieve the carbon neutrality and clean combustion [1] owing to hydrogen characteristics such as being a carbon free fuel [2], high diffusion rate [3], fast laminar flame speed [4], and broad ignition limit [5]. However, there are challenges regarding the use of Hydrogen including the low energy density [6]. The other issue especially for a neat hydrogen engine is the backfire tendency that makes the fuel induction or injection very critical with high NOx amount [7,8].

Different modeling methods of engine are nowadays carried out based on 3D computational fluid dynamics (CFD) [9], 1D simulation of the power system including turbocharger, cooling system, cylinders, and injection line [10], and integration of 1D/3D simulation codes [11,12]. The computational tools allow incorporating fast and targeted machine learning approach to take on the optimisation tasks for selecting the prominent cases that meet the objective function requirement and the defined constraints. It is common to use variety of the 3D topology and shape optimisation to address the design, operation, and injection configuration of the engine such as grasshopper optimisation algorithm [13], design of optimisation (DoE) with machine learning (ML) [14], among other heuristic, and gradient-based optimisers.

Castresana et al. [15] considered a thermodynamic simulation of a single-cylinder engine and used the generated data for the predictive model based on the artificial neural network (ANN). Their obtained results indicated a good prediction accuracy for the brake specific fuel consumption (BSFC) particularly at medium to high loads. The thermodynamic model, on the other hand, is capable of a good system modeling at lower loads. Jena and Tirkey [16] have used the quasi-dimensional modeling of dual-fuel engine while adapting the

* Corresponding author.
*E-mail addresses:* hadi.taghavifar@durham.ac.uk, haditaghavifar@yahoo.com (H. Taghavifar).

https://doi.org/10.1016/j.ijhydene.2025.01.238
Received 25 September 2024; Received in revised form 1 January 2025; Accepted 13 January 2025
Available online 3 February 2025

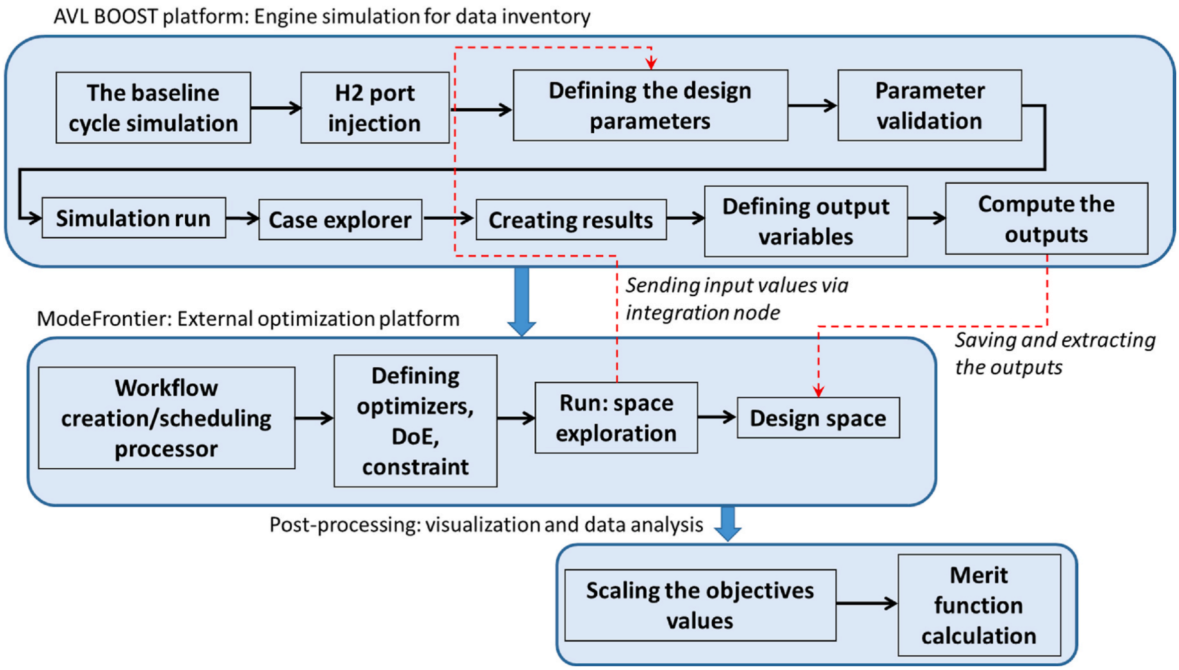


**Fig. 1.** The workflow schematic of two platform interaction and the system optimization by iterative change of inputs and output calculation in the simulation block.

optimisation processing to demonstrate the ideal engine performance. The optimisation was able to determine the recommended valve timing, blending ration of fuels, and intake pressure variation. Recently Wang et al. [17] introduced the multi-objective genetic algorithm optimisation with support vector machine (SVM) to decrease the emission while increasing the economic index. The investigation results indicated successful reduction of fuel consumption along with CO2 and NOx emissions. The works of this type can be referenced for the automatic calibration of the engine function in different operational modes. Taghavifar et al. [18] by using the thermodynamic simulation of diesel/hydrogen dual-fuel reactive controlled compression ignition (RCCI) engine evaluated exergy analysis by variation in combustion duration and compression ratio. The results indicated that the temperature rise, and entropy production can be managed by the compression pressure ratio of the turbocharger. Gautam et al. [19] used a single zone 1D model coupled with a statistical analysis on the combustion phenomena in the cylinder of the engine. The regression analysis and Z-test are employed for the validation that resulted in the assessment of the standard error at different loads and fuel blend ratio. Wang et al. [20] investigated a thermodynamic and exergy analysis of a turbocharged diesel engine with late inlet valve closing possibility. They noted that delaying the intake valve closure together with compression ratio increment can lead to reduction of the irreversibility due to combustion and the exhaust exergy. Chaudhary et al. [21] used response surface method (RSM) to analyze the hydrogen enriched diesel engine with less than 5% error of validation. The application of RSM optimisation with experimental engine tests have been practiced recently in Refs. [22,23] where the input variables are such adjusted to yield maximum power and minimum emission. The mentioned studies lack the novelty of entropy analysis with turbocharged H2 injection and considering the fundamental and updated compressor ratio, H2 injection amount from one side and they also failed to consider advanced scheduler algorithms like game theory and compare its performance with other potent algorithms such as NSGA-II. In the same note, Bae et al. [24] applied multi-objective Pareto optimisation on two-cylinder diesel-ammonia fueled engine to find optimal design points. The applied Pareto front technique proved that exhaust valve timing is more crucial than injection timing in controlling NO emissions and engine performance metrics.

The 1D simulation incorporates the Vibe model for heat release, the Woschni model for heat transfer, and a simplified model for turbocharger simulation considering mean compressor and turbine efficiencies. In this way, it is possible to consider the turbocharger, injection and valve control of different fuel combination more efficiently. On the other hand, the combustion entropy generation, work and power generation can be better monitored as the engine out parameters. In this study, the thermodynamic power system model is connected directly to an optimisation program that processes the 1D modeling results based on input-output parameters to improve the engine operation based on the multi-objective function and the defined constraints. There is few research work devoted on application of game theory and non-dominated sorting genetic algorithm on dual-fuel diesel and hydrogen turbocharged engine. The ability of these optimisers in simultaneous combustion entropy reduction, NO emission decrease, and volume work are compared where the hydrogen fraction and air compression factors as design variables are taken for the engine operation reconfiguration. Observing the case IDs evolutions in each optimisation algorithm gives an important insight from the computational aspect and decreasing the irreversibility and work efficiency by keeping the NO emission in the desired level by adjusting the hydrogen mass fraction and turbocharging performance from thermodynamic modeling are two main contributions covered in this analysis. The flowchart representation of 1D fluid and thermos-chemistry block interaction with optimisation platform in the lower (subsequent) block is illustrated in Fig. 1. The procedures depicted below can organise the methodology and the undertaken steps for the implementation of the research. Three main contributions of this research are.

- The hydrogen port injection and diesel direct injection to combustion chamber and the ratio of fuel in combustion behavior and entropy generation as an indication of exergy destruction has not been fully unraveled and this study paves the way to understand the hydrogen combustion mechanism in a turbocharged environment (compressed air/H2 load).
- Game theory and genetic algorithms have distinct nature of the design space exploration to find the optimal solution. Comparing these schedulers in terms of finding the best trade-off tackling both

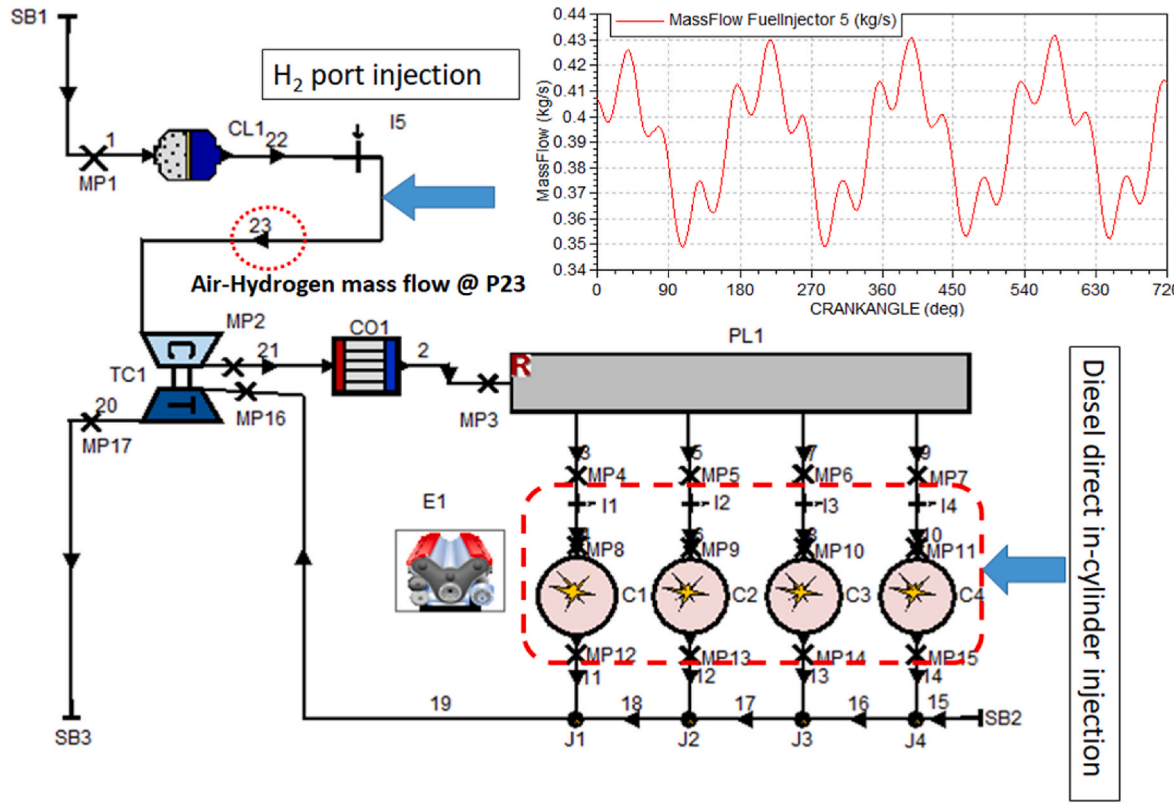


Fig. 2. The proposed propulsion system of a dual-fuel hydrogen-diesel engine with turbocharging effect.

**Table 1**
Modeling parameter in main propulsion system configuration.

| parameters | Value/unit |
|---|---|
| Coolant temperature | 58.2 °C |
| Inlet air temperature | 95 °C |
| Total air cleaner volume | 3.1 litre |
| Number of injector holes | 6 |
| Hole diameter | 0.5 mm |
| Rail pressure | 1500 bar |
| Discharge coefficient | 0.54 |
| Premixed combustion parameter | 0.7 |
| In-cylinder swirl ratio | 2 |

emission reduction and the propulsion system performance in early designIDs is of significance in real-time smart engine operation.

- By online and instant connection of 1D energy system design with AI-based optimisers, the modular platform is created to control the fuel flow and turbocharging to find the best array of inputs conducive to emission minimisation and work output maximisation.

While prior studies have explored optimisation techniques for dual-fuel engines, a direct comparison of MOGT and NSGA-II in the context of diesel-hydrogen engines, considering trade-offs between performance, emissions, and irreversibilities, remains underexplored. This study aims to address this gap.

## 2. 1D propulsion system modeling (engine cycle and gas dynamics)

The propulsion system configuration is demonstrated in Fig. 2 consisting of turbocharger, heat exchanger (cooler), air cleaner, and engine with cylinder arrays. The injection system is a two-step procedure of port Hydrogen injection and direct diesel injection to combustion chamber in pistons. The cyclic air-hydrogen mass flow rate at point P23 is shown and then the charge will be compressed by TC1 into the engine line. The simulation of the flow and combustion is implemented in 1D simulation platform [25] by solving the gas dynamic equations. By adopting the engine cycle simulation, it is possible to consider the turbocharging effect and advanced dual-injection procedure in a propulsion system that is difficult to be performed by 3D combustion chamber simulation. The cycle type is a 4-stroke engine running at 1500 rpm engine speed. The main operating parameters that are used in the modeling in the elements are mentioned in Table 1.

The heat release during the combustion process is simulated according to Vibe model [26] that requires heat release characteristics determined by the shape parameter map, the start of combustion, and combustion duration. The heat transfer in the cylinder follows the Woschni model [27] that considers the surface area and wall temperature of the piston, liner and the cylinder head. A simplified model is chosen for the turbocharger simulation, where engine modeler platform considers the mean compressor and turbine efficiencies over the cycle to compute the energy balance of turbocharging. The calculation procedure is according to the waste gate mode wherein the waste-gate mass flow is calculated from the target pressure ratio across the compressor, the turbocharger efficiency and the specified turbine size. The flow type is discharging coefficient to account the swallowing capacity of the turbine. In this way, the effective flow area of the turbine is calculated from the equivalent discharge coefficient and a turbine reference area.

The initial model is configured with a direct injection of diesel to cylinders. The main component as elements is considered in the working directory and connected (the measuring points in underlying sections are added to monitor the flow characteristics). The operational condition values are defined within each element. In a modified version, the turbocharger is incorporated while the system is retrofitted with hydrogen port injection so that both hydrogen and air will be compressed for effective combustion. The baseline case with the associated input variables is introduced as a case study and the resulted system performance are displayed with in-cylinder pressure, H2 and NO mass

**Table 2**
The input variables with the variation limit, central value, and delta value.

| Name/input | Lower bound | Upper bound | Central value | Delta value |
|---|---|---|---|---|
| H2 inj. Mass (kg/cycle) | $1.9 \times 10^{-5}$ | $2.9 \times 10^{-5}$ | $2.4 \times 10^{-5}$ | 5.0 |
| Turbocharger efficiency (%) | 57.57 | 93.63 | 75.6 | 18.03 |
| Compressor pressure ratio (−) | 1.1 | 3.0975 | 2.09875 | 0.998 |
| Start of combustion (CA deg) | −12.075 | 0.0 | −6.0375 | 6.0375 |

fractions.

In diesel engines, the combustion characteristic depends strongly on the capabilities of the fuel injection system, compression ratio and the charge air temperature. The combustion duration is approximated based on the crank angle interval between 10% and 90% of mass fraction burned. The calculations for the baseline model are conducted and the design variables bound for the optimisation task is determined according to Table 2 with the specified statistical information.

The NOx emission is based on Pattas and Haefner model [28]. All reactions rates of the Zeldovich mechanism $r_1$ to $r_6$ are used in the NO concentration assessment. Meanwhile, the concentrations $c_i$ are molar concentrations under equilibrium conditions with units [mole/cm$^3$].

The NO generation as aftermath of combustion in the cylinder in [mole/cm$^3$s] is calculated as:

$$r_{NO} = C_{Post\ Pr\ ocMult}.C_{KineticMult}.2\left(1-\alpha^2\right).\left(\frac{r_1}{1+\alpha AK_2}+\frac{r_4}{1+AK_4}\right) \tag{1}$$

Where $C_{PostProcMult}$ and $C_{KineticMult}$ are the modular parameters controlling the post-processing and reaction kinetics. Other parameters specified in above equation are as follows:

$$\alpha = \frac{c_{NO,act}}{c_{NO,equ}} \times \frac{1}{C_{KineticMult}} \quad AK_2 = \frac{r_1}{r_2+r_3} \quad AK_4 = \frac{r_4}{r_5+r_6} \tag{2}$$

The Zeldovich mechanism assumes that the NO production depends on the reaction constants, temperature, and species concentration in a series of stoichiometry reaction pathways.

After the simulation and creation of series results, the response editor connects to external optimiser to handle the optimisation of the power system.

The simulation results for the system in terms of heat release rate, in-cylinder pressure, and temperature profile are shown in Fig. 3. The modeling data can closely match with experimental measurement data [29], which confirms the reliability and reproducibility of valid information with 1D thermodynamic representation. Both obtained results are based on diesel fuel test in the experimental and numerical modeling at full load operation under 1500 rpm engine speed. The highest discrepancies occur around 360 CA for HRR and pressure traces since the injection and ignition models are activated during the simulation procedures. In the temperature profile, however, the highest deviation from experimental data takes place at post combustion period after 540 CA where the exhaust gases are depleted from the cylinder.

## 3. Optimisation process

By specifying any inputs in the designed system, a case explorer is created and by running the model a set of responses is calculated. However, to collect data, the simulated system is connected to a scheduler platform in online format that organizes the model input feed systematically based on optimization algorithms. In this method, a design space consisting of possible solutions are produced as a large dataset arranged in the format of input/output series. The optimisation algorithms as the processing units take control of the engine model and command how to change the selected input variables. The resulted data points are stored in the designated tables with Pareto solutions. The optimisation interface handles the configuration of parameters and running the power system simulation to obtain the results. The structure and the workflow representation of the optimisation platform along with inputs/outputs, and constraints are shown in Fig. 4. The used platform for optimisation is capable of the system analysis with data processing and the system performance upgrade.

The Design Objective Nodes are target terminals characterizing numeric variables computed in the Data Flow as a function of input or/and output parameters and used as optimisation objectives. In the node configuration, the design of objective parameters with respective weights is possible. The objective function is configured according to following expression with the aim of minimizing NO emission and entropy while maximizing the VolWok:

$$F = \sum_{i=1}^{n} w_i F_i = w_1(VolWork) + w_2(NO) + w_3(Entropy) \tag{3}$$

where $w_1$, $w_2$, and $w_3$ are the designated weights for sub-objective parameters of VolWork, NO, and entropy. Two sets of weights are recognized in this study for both optimisation algorithms to monitor the effect of significance of different factors in the optimisation goal.

The process of data transfer within the integrated powertrain model and the optimisation interface is as follows.

1. Optimisation platform [30] sends input values via an integration node to the connected powertrain system.
2. The virtual twin model uses the input values to compute the outputs of the system.
3. The optimiser extracts output values and saves them in the Design Space.
4. These steps are repeated for each design.

The following steps are taken to implement the data scaling or data normalisation based on the range function to avoid domination of variables with a high numerical range on the results.

- Dataset selection: A table containing the Pareto designs would be served as training data.
- Exclude data: The unfeasible and erroneous data from the population would be removed.
- Scaling function: There are options for scaling including range, variance, logarithmic, and logistic for scaling. The range function will be applied on the data.

### 3.1. Design of experiment

To avoid multiple test cases in experimental research, a preliminary design space exploration is carried out in numerical investigation. The initial sampling of design space, which can be performed manually or automatically is called design of experiment (DoE). The DoE initialized space is beneficial in identifying the most influencing factor as well as understanding the relationship between the variables. For optimisation purpose, DoE allows to start with a desirable starting population. In this research, for genetic algorithm optimisation, the uniform Latin Hypercube (ULH) stochastic DoE is selected with 11 number of designs since it matches well with NSGA-II. This type of input generation tries to minimise the correlation between the input variables and maximise the distance of the generated designs in the design space [31]. For the MOGT optimisation algorithm, 10 space filler randomly chosen population of input variables are used for initial sampling of the optimisation process.

### 3.2. Multi objective game theory (MOGT) optimisation

This algorithm is based on game theory, which is efficient in highly

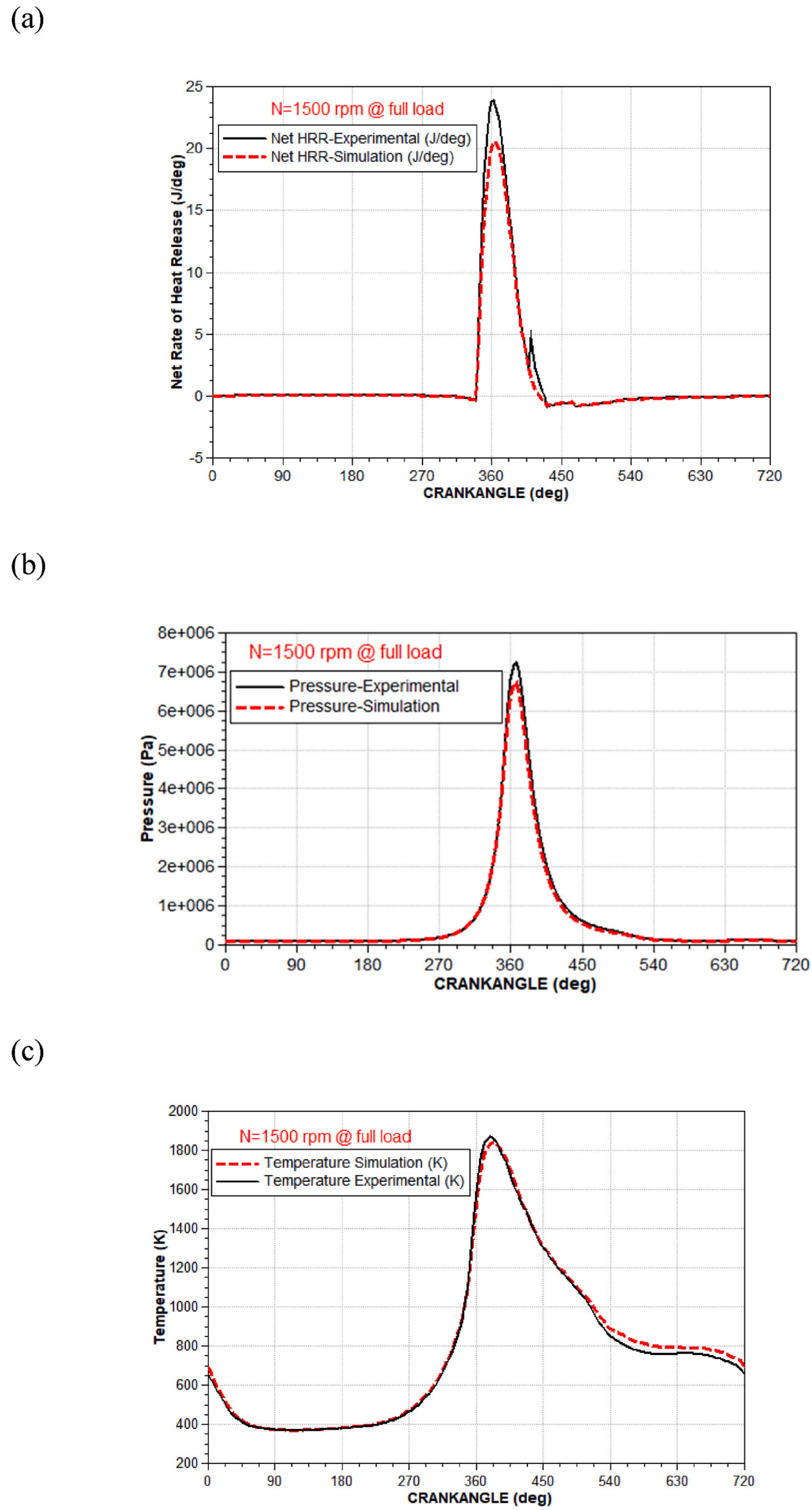


**Fig. 3.** The validity of simulation results at 1500 rpm engine speed and under full load operation condition: (a) net heat release rate, (b) in-cylinder pressure, and (c) in-cylinder temperature.

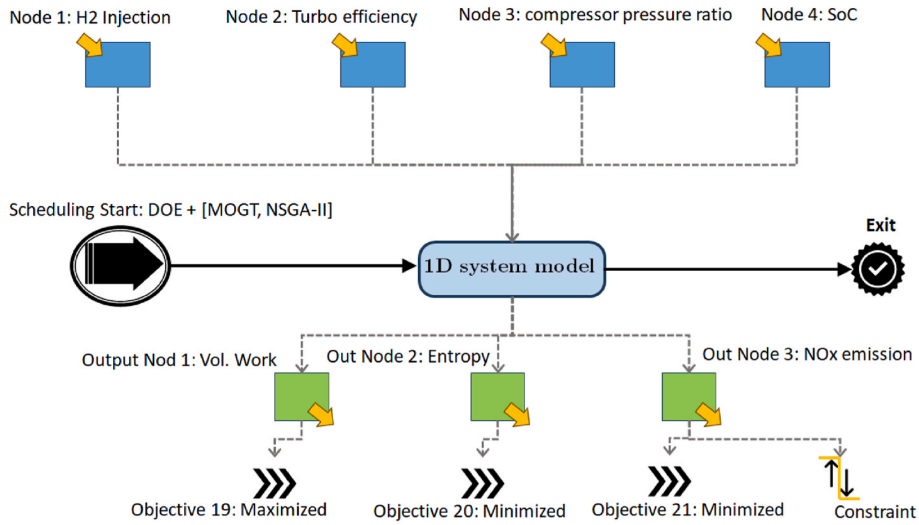


**Fig. 4.** The optimisation platform with objectives, design variables, constraint on NOx, and the processing technique.

**Table 3**
The MOGT main parameters tuning and the algorithm configuration.

| Parameters | Values/method |
|---|---|
| Maximum number of players steps | 10 |
| Simplex maximum number of iterations | 6 |
| Final termination accuracy | 0.01 |
| Maximum number of designs for screening | 500 |
| Variable screening method | Smoothing spline ANOVA |
| Variable-objective assignment criterion | Max. Variance |

non-linear and constrained problems [32]. It mimics the competition game between players and each player has the task of the assigned objective optimisation. It is necessary that the objective numbers be less than the input variables. This optimisation algorithm is categorized among heuristic optimisers. In the MOGT algorithm, each player is responsible for an objective and the design space or input variables are randomly given to players. Now, every player tries to optimise the assigned objective by variation of the inputs (during the initial phase, other variables are kept fixed with DoE values). In this step, the Simplex method is employed for the single-objective optimisation. Next, each player renews the values of their input variables and delivers to other players, substituting the initial DoE values with updated best values for the considered objective. In this manner although the players follow their own objectives, they are limited by the input values found by others.

Finally, each step players exchange variables assigned to them. If the variable is not significant (the objective function is not changed notable with its variation), it is assigned to another player, in the next stage. Variables can also be randomly exchanged if they are equally important for all objectives. The result of the game is the Nash equilibrium [33], which means no player can benefit from changing their strategy while the other players keep theirs unchanged. MOGT starts with the initial set of DoE table, while other entries are skipped. During the simplex initialisation, n+1 first designs are used where n is the number of input variables. The algorithm terminates once the maximum number of player steps is reached, or the desired accuracy is established. This algorithm features automatic decomposition of the variables space among the players (in charge of each objective). It also allows concurrent evaluation of configurations proposed by each player. Table 3 summarizes the key tuning values and parameters configurations. The maximum number of MOGT evaluations can be estimated by the following equation:

$$evaluations = 1 + [\mathrm{y} \times (\mathrm{simplex\_iteration} + 1) + x] \times \mathrm{player\_steps} \quad (4)$$

where x and y are the number of input variables and objectives.

Max. Variance is a deterministic approach that is adopted as a criterion for the results of analysis of variance (ANOVA) analysis. In this way, the significance of each input variable for each objective is computed. The algorithm picks the variable with the highest significance and assigns it to the given objective. The maximum number of players signifies the maximum decision steps or iterations that a player can adopt in the game optimisation procedure. Furthermore, the smoothing spline method assesses the significance degree of each input on output or the objective, thereby the variable prioritisation is implemented. Considering players $P = \{P_1, P_2, \ldots, P_n\}$, where n is the number of players or the objectives, and the strategy profile $s = \{s_1, s_2, \ldots, s_n\}$ (each $P_i$ chooses $s_i$ from a strategy set), then a multi-objective utility vector can be defined as [34]:

$$U_i(s) = \left(U_i^1(s), U_i^2(s), \ldots, U_i^m(s)\right) \quad (5)$$

where m is the number of objectives. In this sense, each player denoted by Pi tries to optimise the entrusted utility vector Ui (i.e., Pi: max. Ui(s)). The assigned pareto optimal strategy solutions are s*, therefore:

$$U_i^m(s) \geq U_i^m(s^*) \quad (6)$$

Meaning that the utility of a player cannot be improved unless another player's utility being decreased for at least one objective.

### 3.3. Non-dominated sorting genetic algorithm II (NSGA-II) optimisation

This method of optimisation is implemented in the optimiser platform, which is developed at Kanpur Genetic Algorithm (KanGAL) [35]. This type of algorithms is typically time demanding particularly when the population size is big. However, keeping the population diversity is an important privilege of genetic algorithm. This algorithm consists of two operators, namely mutation and crossover. The NSGA-II can manage both continuous and discrete variables and the constraints are treated with the constraint domination technique. The constrain domination technique handles the constraints in the following manner.

- Pareto dominance criteria rank the feasible designs
- Feasible designs are ranked higher than unfeasible designs
- If sum of the constraint violation for a design is lower than other unfeasible designs, then it is ranked higher

**Table 4**
performance metrics of NSGA-II and MOGT.

| | Total designs | Error designs | Unfeasible designs | Best ID convergence | DoE |
|---|---|---|---|---|---|
| NSGA-II | 100 | 25 | 16 | ID95 | Self-initialized (11 population) |
| MOGT | 100 | 17 | 28 | ID92 | User (10 population) |

Three algorithm variants are introduced in the used algorithm that enhances the performance of original NSGA-II: 1) the controlled elitism to promote the exploration in the design space and enhance the uniformly distribution of solutions, 2) the variable population size that enables more accurate searching, 3) the magnifying front genetic algorithm (MFGA) [36] variant that combines the steady-state evolution with the adaptive elitism to effectively use the computational resources. For this optimizer the self-initialising mode is opted which automatically adjusts the DoE and configuration of the algorithm. This means that GA operators and the algorithm configuration is performed according to the defined data characteristics and optimisation goal.

The computation is rendered with Intel(R) Core i7 @ 1.8 GHz computer. The average time of 1D computation with the engine setup platform is 2 m:17s for MOGT whereas the average time of calculation for each case in NSGA-II is 1 m:44s depending to the complexity of problem. The entire optimisation duration for the total cases is 2h:50 m:38s and for NSGA-II optimisation with number of cases (solutions), the total elapsed time is 2h:32 m:26s. This shows that NSGA-II succeeds in less computation and processing cost compared to MOGT, although MOGT outperforms in finding more optimal result in early case number.

## 4. Result and discussion

After simulation of the turbocharged propulsion system fueled with hydrogen-diesel and connecting the obtained data to scheduler program to perform the advanced optimisation, the comparison is implemented between two algorithms with different nature of searching in the design space. The target of the study is to maximise the work volume while

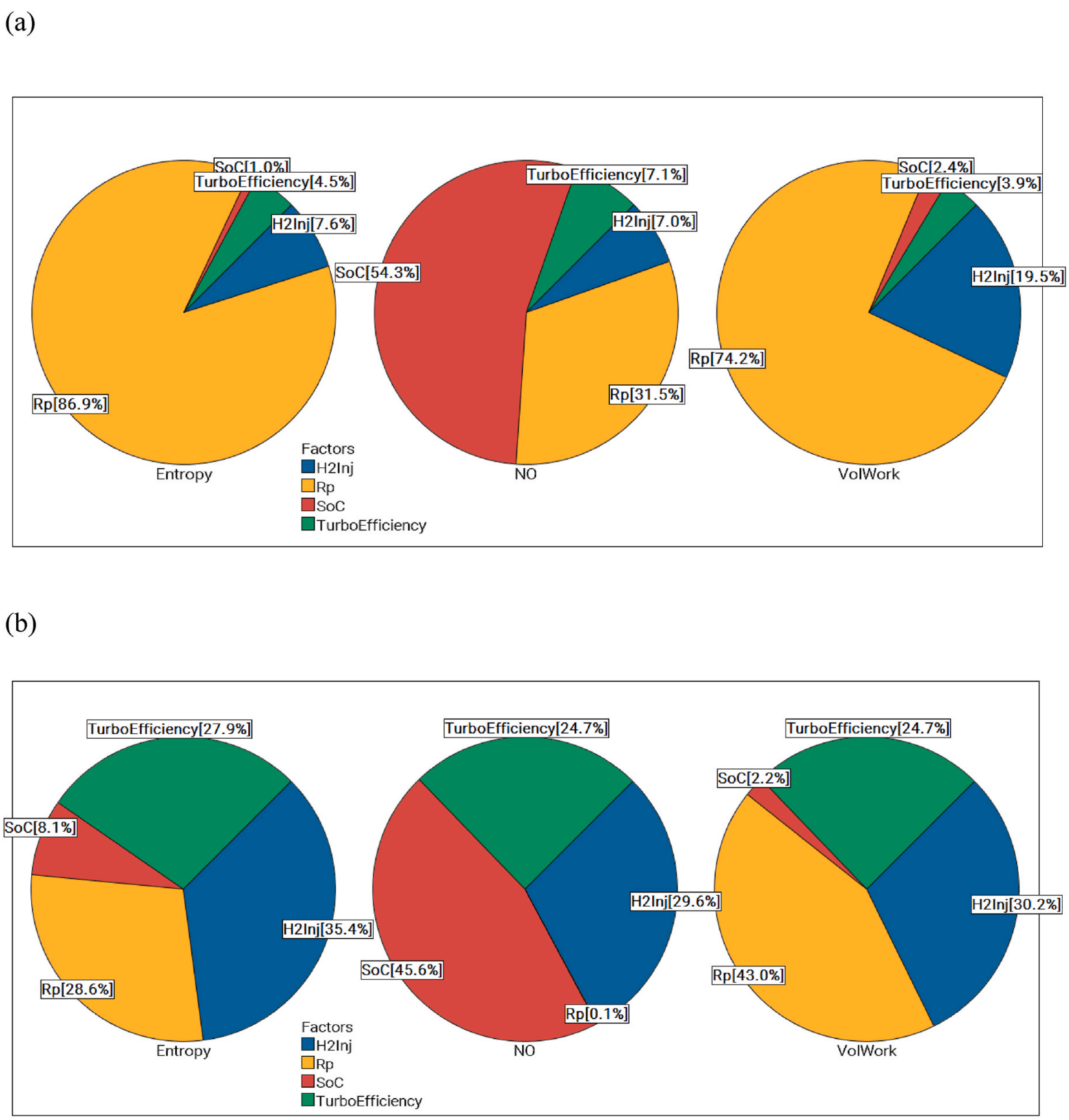


**Fig. 5.** Overall student chart based on input variables for three objectives of the optimisation: (a) NSGA-II and (b) MOGT.

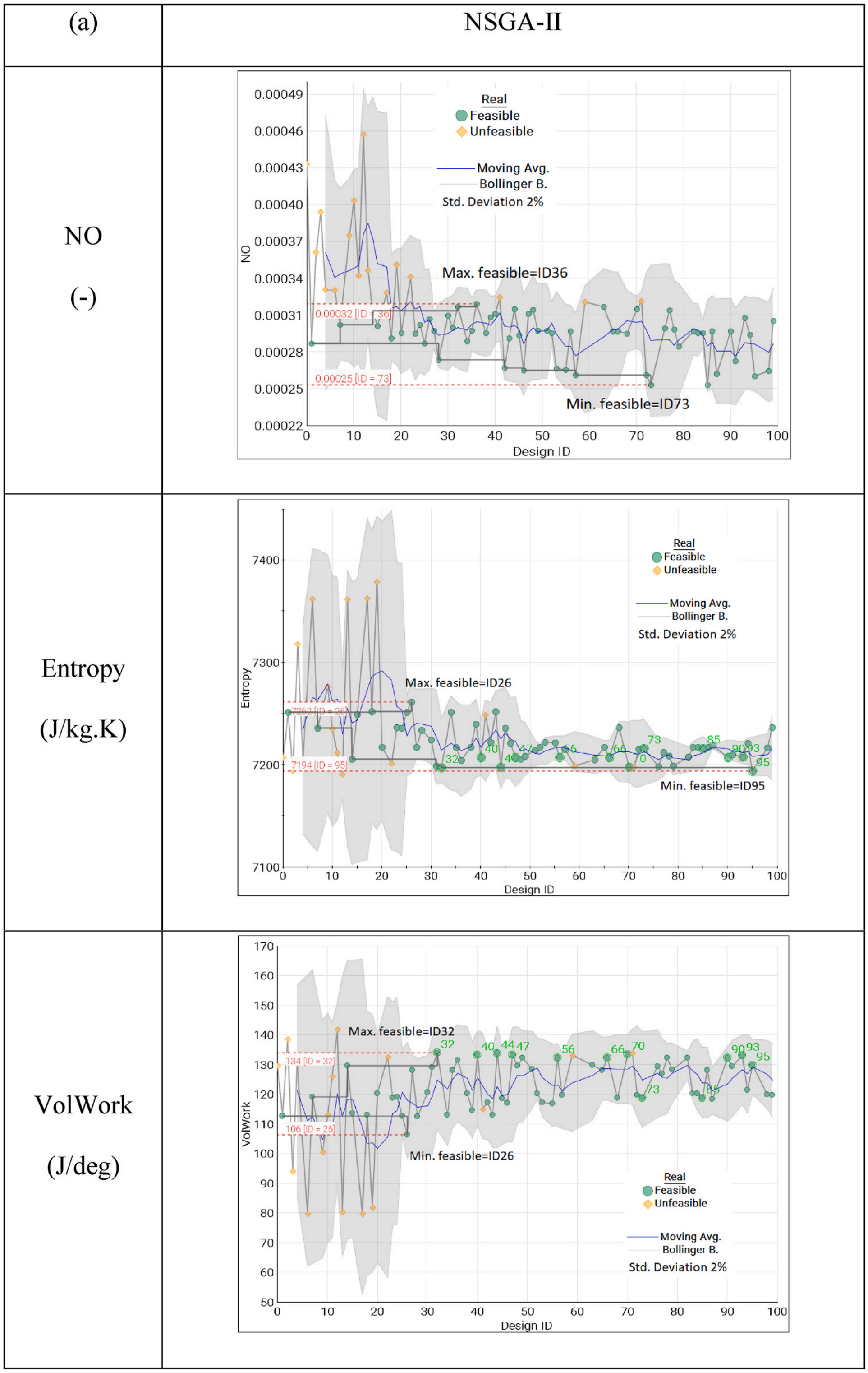


**Fig. 6.** The history plot of objectives evolution with 100 population size: (a) NSGA-II, (b) MOGT.

maintaining the minimal entropy and NO emission. This is planned by variation of input parameters in the powering design including the start of combustion, Turbocharger efficiency, hydrogen injection mass, and the compressor pressure ratio. In the optimisation process, there is a constraint imposed on the NO limit (NO mass fraction $<3.2 \times 10^{-4}$) to recognize the feasible and infeasible solutions. The results of optimisation by two methods are mentioned in Table 4. The MOGT is faster in finding its best solution with less error designs, however, suffers from more unfeasible solutions that do not observe the NO constraint (the best design ID is introduced based on higher merit function values).

The importance of the selected inputs on different objectives are exhibited in the overall student pie chart in Fig. 5. As shown, NSGA-II

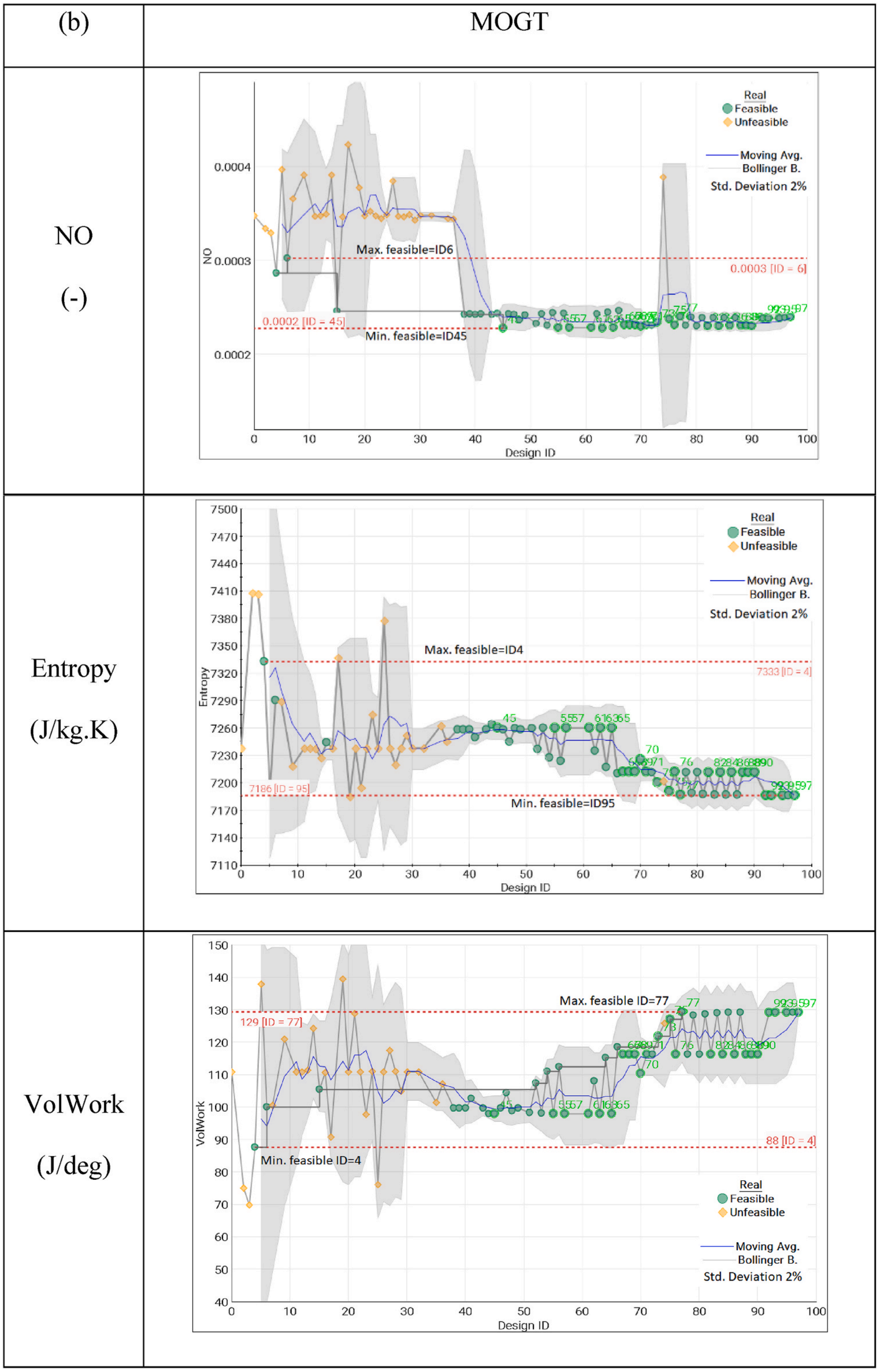


**Fig. 6.** (*continued*).

and MOGT show different significance of inputs, however the joint trend can be observed between two scenarios. For instance, the SoC is a dominant factor on NO in both optimisers with 54.3% and 45.6% significance share in NSGA-II and MOGT, respectively. The reason is that combustion start greatly influence the flame temperature and overall kinetics of the reactions leading to $N_2$ bound breakdown. The compressor pressure ratio is a leading element in the work volume and higher compression pressure causes more work delivery as the piston work formula suggests ($W = \int Pdv$). In a general view, the compressor pressure ratio plays a highlighted role on the objectives, whereas for MGOT, the H2 injection and turbocharger efficiency are more paramount in variation of the three objectives.

The performance of each of optimiser types in generation of objectives during 100 evolutions are shown in history chart of Fig. 6 in

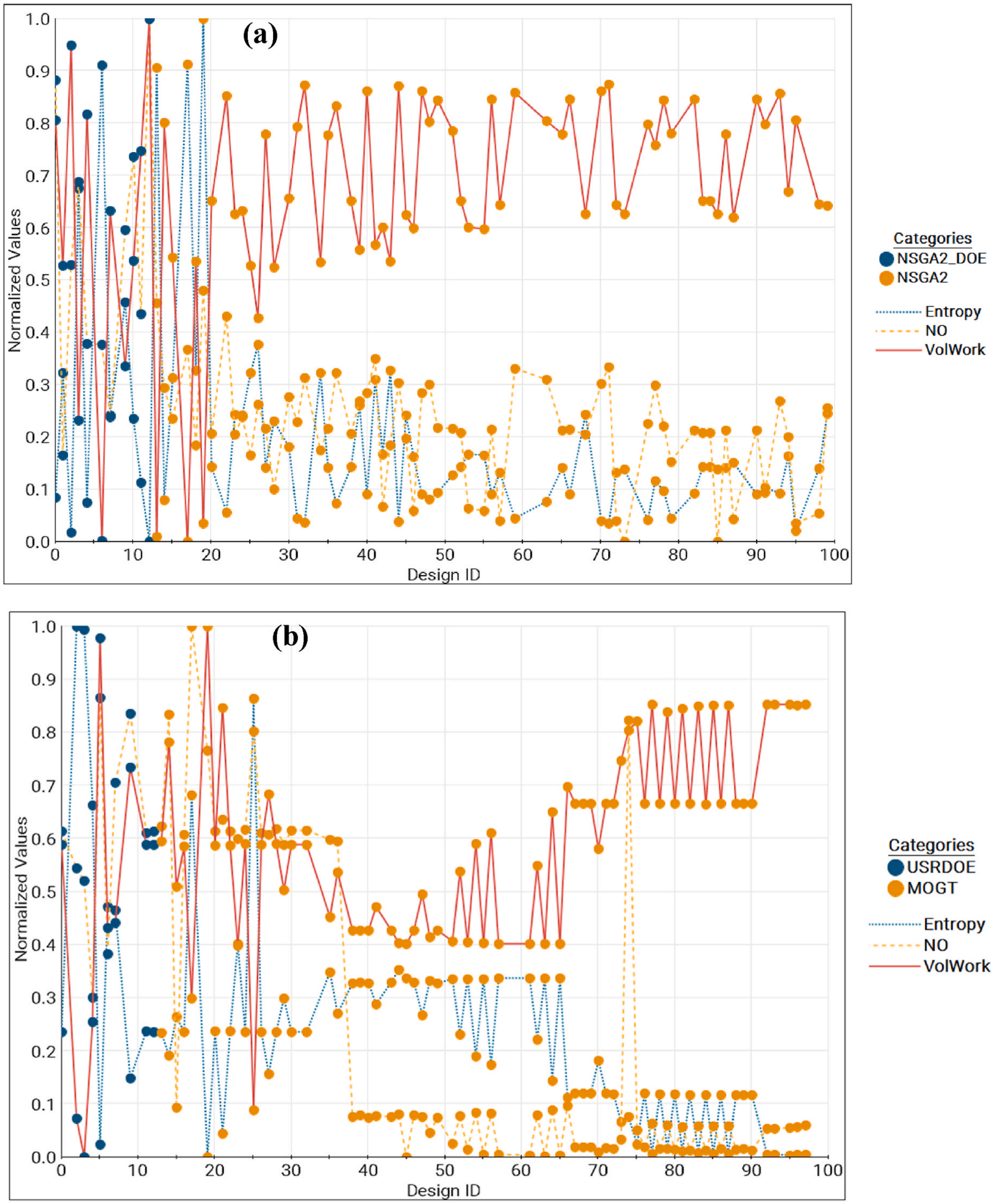


**Fig. 7.** non-dimensional objectives variation with DoE initial designs (a) NSGA-II and (b) MOGT optimisation algorithms.

**Table 5**
Baseline and optimal elite cases specs.

| | Baseline case | NSGA-II (ID95)[a] | MOGT (ID92)[a] |
|---|---|---|---|
| H2 inj. Mass (kg/cycle) | $2 \times 10^{-5}$ | $2.17 \times 10^{-5}$ | $1.9 \times 10^{-5}$ |
| Turbocharger efficiency (%) | 60.6 | 76.7 | 61.98 |
| Compressor pressure ratio (–) | 2.95 | 3.0 | 3.0975 |
| Start of combustion (CA deg) | −11.5 | −1.18 | −0.017 |

[a] NOx mass fraction constraint $<3.2 \times 10^{-4}$.

detailed 2% std. deviation band, min/max limit, feasible/unfeasible solutions categories. It is interesting to observe each algorithms' potential in maximizing or minimising the objective output. First in the DoE initial phase the domain of variation is extensive and then in later generations they are narrowed down. For NSGA-II, the evolutions are more periodic, while for MOGT the variations are more structured and fluctuate in equal band and then a drastic change occurs. The mean average line (blue line) can better illustrate the evolution of suggested outputs during the produced population. If the target is maximising an objective, this line gradually rises and if the target is minimising, the average line gradually declines. The minimum NO value is reached at ID73 for NSGA-II but the lowest NO is achieved at ID45 which is lower

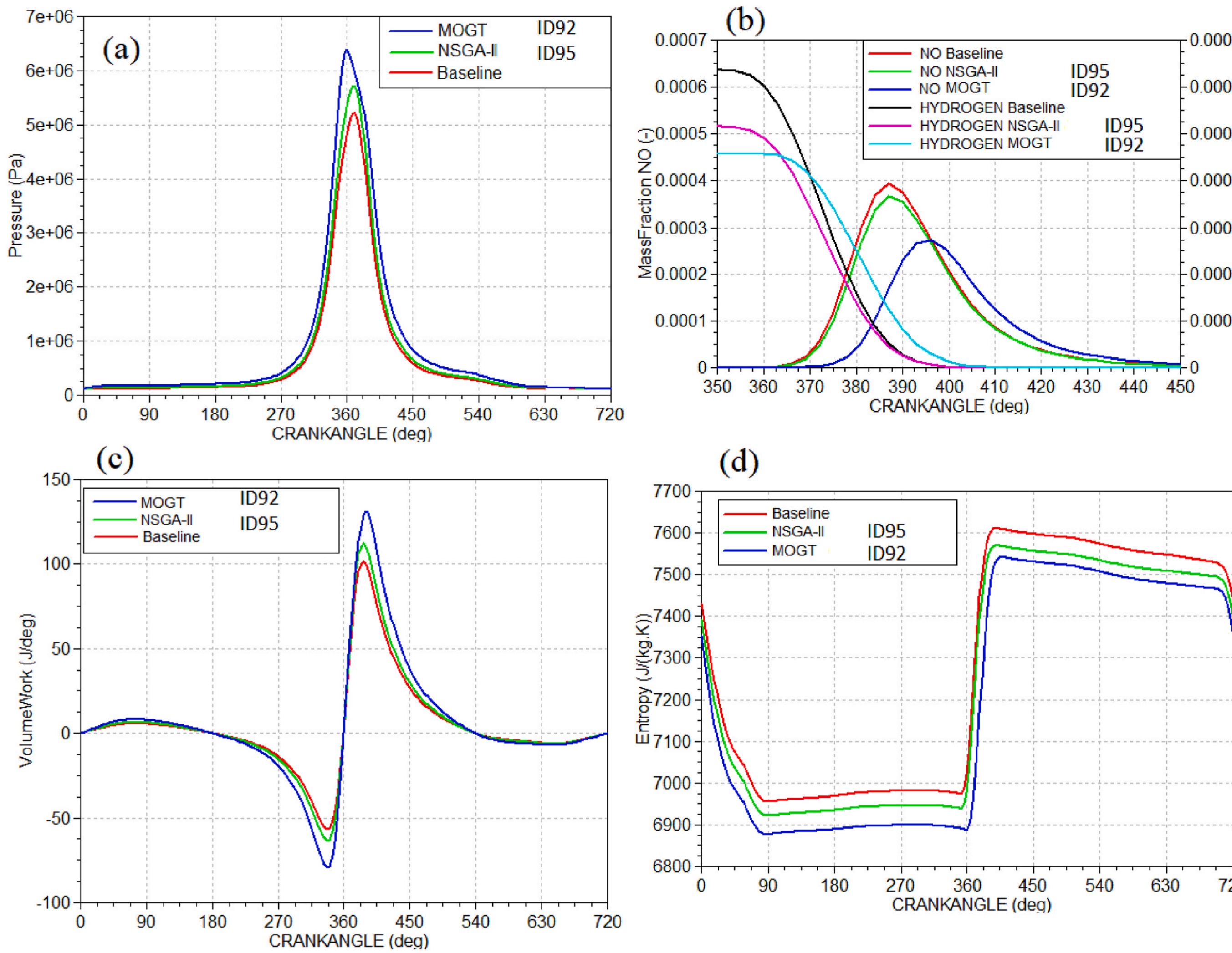


**Fig. 8.** The variation of (a) pressure history, (b) NO and H2 mass fraction, (c) volume work, and (d) entropy for baseline case, MOGT ID92, and NSGA-II.

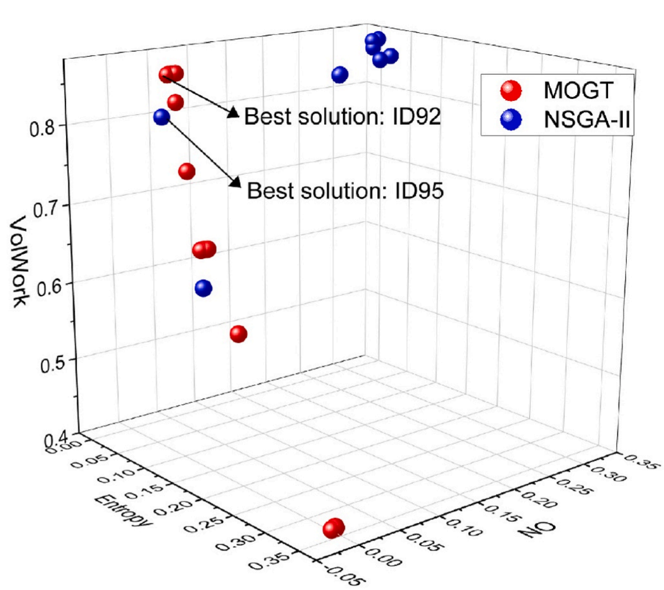


**Fig. 9.** The Pareto front solutions scattered in 3D for MOGT and NSGA-II optimisers.

than genetic algorithm solution for NO minimization. Both optimiser find the minimum entropy at ID95, however the value found by MOGT is 7186 J/kg.K that is below the entropy by the NSGA-II (7194 J/kg.K). The third objective is work volume that NSGA-II shows better performance in finding the maximum work amount since it finds the maximum work (134 J/deg) at ID32 compared to MOGT, which introduces the best solution at ID77 with corresponding work amount of 129 J/deg. This confirms that MOGT is more successful than NSGA-II in searching and speed in minimising NO and entropy. It is also important to note in the trend pattern of the series evolution for the responses between two optimiser algorithms.

The scaled (normalised) values of objectives in the range of 0–1 as evolved in the design space are displayed in Fig. 7 for NSGA-II and MOGT optimisation algorithms. The variation of input variables is performed by optimisation algorithms and during the initial DoE population, the variation of responses for entropy, NO, and VolWork are large and random. However, in the subsequent designs the gap or variation band are narrowed, and a more structured variation can be observed. The variation pattern of objectives between two optimisers (NSGA-II: evolutionary vs. MOGT: heuristic) show their strategies in searching within the design space and finding the best solution. The non-dimensional objectives can better represent the variation of each objective in comparison to other objectives. Two objective functions represent different weighting or significance of each parameter i.e. NO, Entropy, and VolWork. NO and Entropy are set to be minimised while

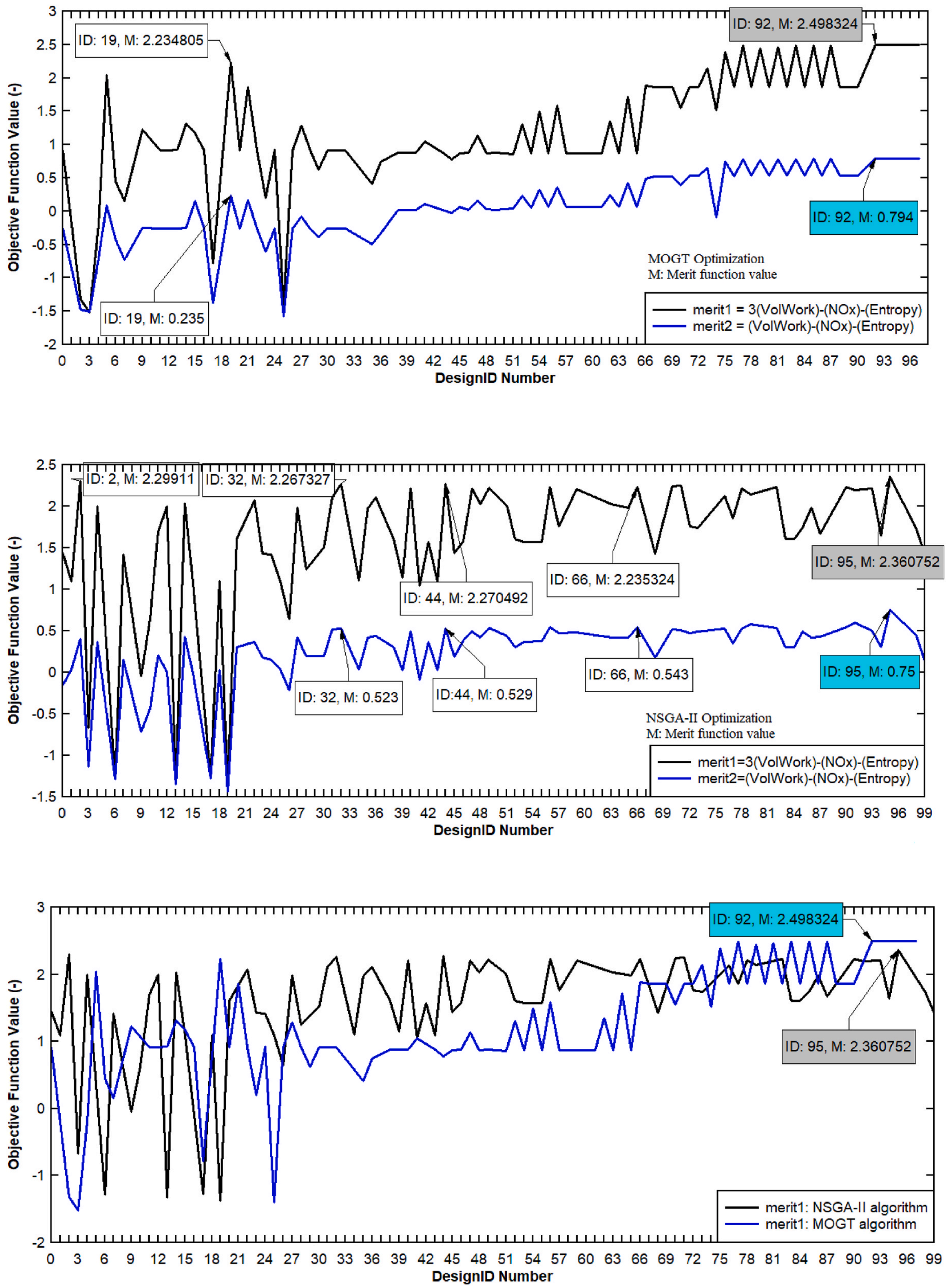


**Fig. 10.** Objective function variation for two different algorithms of MOGT and NSGA-II based on two merit functions.

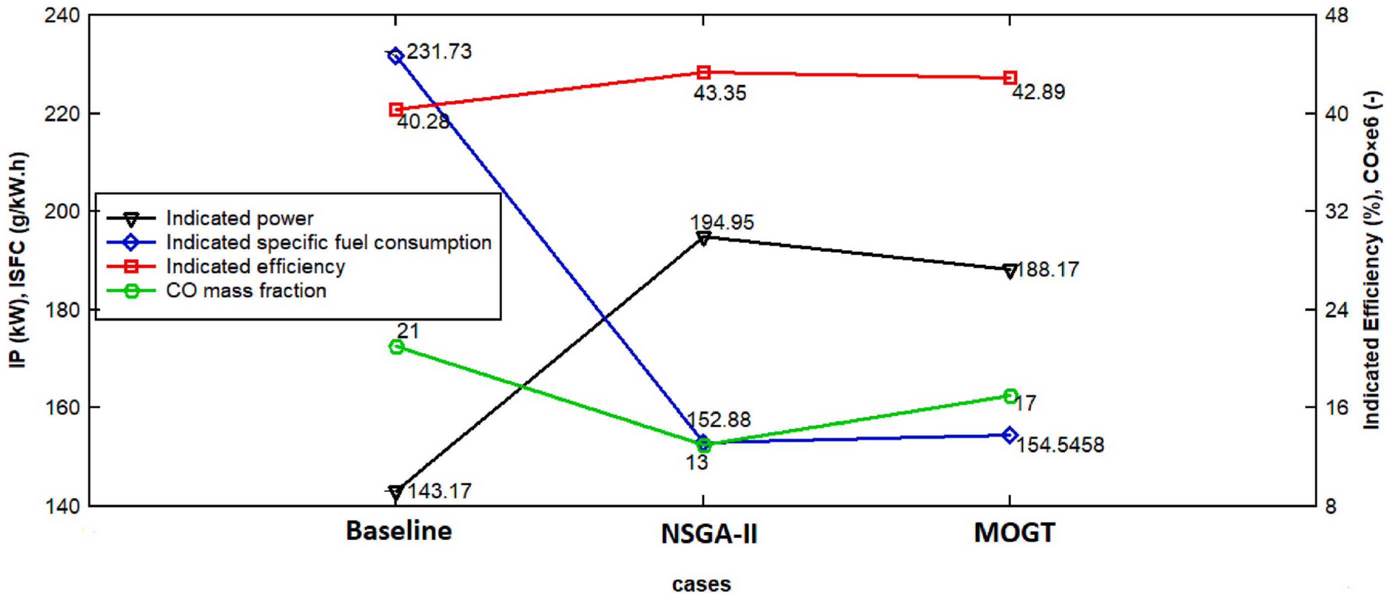


**Fig. 11.** Comparison of IP, ISFC, efficiency, and CO between the base case, NSGA-II, and MOGT cases.

VolWork is designated to be maximised as the goal of optimisation. In addition, we can define the merit function or multi-objective function based on different weights and scaled objectives of entropy, NO, and VolWork. In this regard, two merit functions are defined as:

$$\begin{aligned} &Merit\_function1 = 3(VolWork) - (NO) - (Entropy) \\ &Merit\_function2 = (VolWork) - (NO) - (Entropy) \end{aligned} \tag{7}$$

The best results or solution obtained for the optimisation algorithms to maximise the delivered work and at the same time minimise the entropy and NO emission are ID92 and ID95 for MOGT and NSGA-II, respectively. Each algorithm manages the variation of inputs in a unique way to reach the desired objective function amount. For example, as the H2 injection increases the entropy for MOGT, the hydrogen injection amount cause entropy reduction based on NSGA-II. In some cases, both algorithms suggest that SoC has the biggest inverse effect on NO emission. This is an indication that variation of inputs may lead to different results in the objective function value for different optimisation algorithms. To have a better vision on the input values for three categories of the baseline case (with no optimisation), the best NSGA-II solution (ID95), and the best MOGT solution (ID92), Table 5 is provided. This table confirms that to achieve the objectives, the SoC should be retarded to top dead center (TDC) timing. This contributes towards reduction of NO emission formation once we shift from −11.5 °CA to either −1.18 °CA or −0.017 °CA. However, the SoC has the least influence on entropy or work amount. On the other hand, the H2 mass injection impacts the results contradictorily since a higher hydrogen injection (compared to the base case) led to the best result according to NSGA-II, while a lower hydrogen mass yielded optimal response with MOGT. Both scenarios suggest that if H2 injection increases then the NO emission amount increase since the chamber temperature increase. The hydrogen injection affects the entropy and volume work differently such that H2 mass increases the entropy based on MOGT, while it can decrease entropy according to NSGA-II. According to Table 4 both input parameters of turbocharger efficiency and compressor pressure ratio have a direct effect on the objective solutions with different effect sizes. This duality of optimisation algorithms behavior with input parameters mainly originates from the nonlinearity and the complexity of the generated data and the combustion process with diesel and hydrogen.

The pressure, NO and H2 mass fraction, volume work, and entropy histories are represented for the baseline case, MOGT optimal case, and NSGA-II optimal case in Fig. 8. As shown, the optimisation scheduler was able to enhance the pressure generation based on the proposed input parameters. The best case generated by MOGT is more successful than that of NSGA-II optimisation program and both pressure of the cylinder and the volume work peaks are higher for MOGT ID92. By applying the MOGT 18.2% more pressure peak can be achieved compared to the base case. The hydrogen mass fraction profile and the NO variation can better illustrate when hydrogen mass is dominant, the NO emission is accordingly higher compared to other cases. Under adopted measures for input parameters for ID92 of MOGT scheme, it is possible to keep the entropy the lowest and this helps for exergy destruction (irreversibility) minimisation during the fuel injection, air compression, air-fuel mixing, combustion, and post-combustion phases. The entropy amount is tried to be reduced to prevent the energy dissipation and try to recover the exhaust gases energy as much as possible. The MOGT tries to achieve the low entropy by lower hydrogen injection, since hydrogen makes a high-temperature combustion where the energy can be dispersed during the combustion or transported by the exhaust gas through the respective port/manifold. Minimising the entropy generation has always been a practical goal in the engine design that the optimization program could accomplish by manipulation of the start of combustion, hydrogen injection amount, and turbocharging effect.

The Pareto front solutions for both MOGT and NSGA-II optimisers are displayed in 3D scatter plots in Fig. 9. The distribution of selected Pareto shows that NSGA-II is focused on increasing the VolWork, while majority of the proposed solutions lie on relatively high NO (>0.25 normalized value). MOGT, on the other hand, shows a better distribution of the Pareto solutions that stay in low NO and entropy zone (the best solution found by this algorithm gives high VolWork). Comparing the best solution IDs by these two algorithms show that they are in vicinity of each other in the 3D objective space each having their own pros and cons. It must be noted that the number of Pareto solutions for MOGT is higher than NSGA-II, which is a better MOGT performance indicator.

The overall performance of the optimisation algorithms for two merit functions during the 100-population evolution is displayed in Fig. 10. The way the objective function amount varies for MOGT and NSGA-II are exclusive and shows how they perform to find the optimal solution while observing the constraint. The local optima in the initial search space occurs at ID19 for MOGT with $M_1 = 2.23$ and $M_2 = 0.235$ while further attempt and exploring other regions lead to a gradual average increase from ID52 and finally at ID92 the optimiser succeed at finding the global optima with $M_1 = 2.49$ and $M_2 = 0.79$ ($M_1$ merit function emphasizes more on the work output from the piston). Regarding the

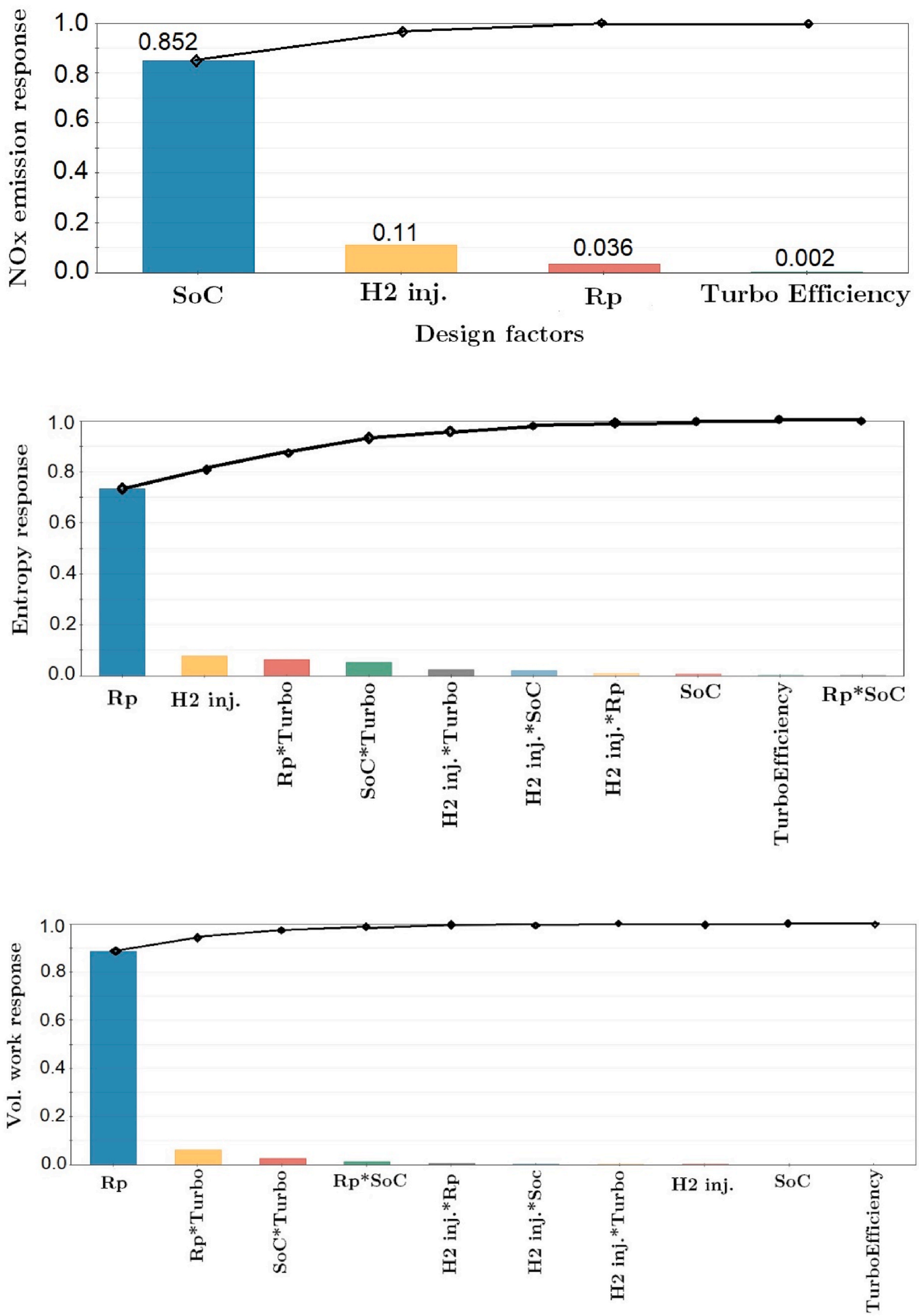


**Fig. 12.** The sensitivity analysis performed with SS-ANOVA method for response outputs.

**Table 6**
Comparison of the study with a peer study results, methods, and scope.

| | Engine method | Fuel injection | optimisation | results | comment |
|---|---|---|---|---|---|
| This work | 1D turbocharged | Hydrogen port/ Diesel direct | DOE + MOGT/ doe+nsga-II | Work, entropy and NOx | This work features turbocharged, combined port/direct injection. Entropy as an indication of irreversibility is integrated and two advanced optimisers are compared and analysed. |
| Salek et al. [37] | 1D gasoline engine | Hydrogen/gasoline port injection | DOE + GA | NOx and brake mean effective pressure | The water injection effect is analyzed |

NSGA-II optimizer, the objective function from the starting population introduces high values but in the subsequent cases from ID20 onwards, the minimum objective values disappeared, and we have several local optima. Finally, the algorithm can find the global optimal point with the highest objective function value at ID95 corresponding to $M_1 = 2.36$ and $M_2 = 0.75$.

Comparing two methods of optimisation reveals that MOGT is faster in finding the best solution with the highest objective function value $M_1$ (MOGT) @ ID92 = 2.498 > $M_1$ (NSGA-II) @ ID95 = 2.36. Each algorithm has its own way to modify the propulsion system configuration to satisfy the objectives for example MOGT tries to control the hydrogen injection ratio while NSGA-II increases the turbocharging efficiency and boost the compression ratio of the air. The comparison of two algorithms merit function values demonstrates that between ID27 until ID67 the NSGA-II shows better results with higher objective value but afterwards in the end cases MOGT becomes dominant in the competition.

Fig. 11 is presented to compare baseline, NSGA-II, and MOGT cases in terms of other engine metrics than included in the objective function consisting of the indicated power (IP), indicated specific fuel consumption (ISFC), indicated efficiency, and CO mass fraction. The results show that the optimisation can significantly increase the power of the engine and indicated thermal efficiency while CO emission and fuel consumption are reduced. However, it can be noted that for these parameters, NSGA-II solution outperforms the MOGT solution. This means that if MOGT solution is more successful in NO reduction, NSGA-II optimal case can lead to a lower CO emission. Although the volume work of MOGT is higher than NSGA-II, the produced power and efficiency of NSGA-II is comparatively higher. This is due to the combustion efficiency and timing that are different for two methods of optimisation. In NSGA-II, there is higher rate of hydrogen injection that leads to lower CO but higher NO at the same time. This shows that the optimisation cannot necessarily present a universal solution that meets all performance metrics, however, we can determine which factors are of more significance and priority and which limit can be set as the constraint for the feasible solutions.

The sensitivity analysis is conducted to identify the most important input variables by evaluation of main and interaction effects of factors on selected responses. The effect of single factors are explored on the NOx emission objective, while the interacted factors are added for the sensitivity of entropy and work outputs (since Rp is the most dominant and others are very low). The sensitivity analysis employs smoothing spline ANOVA (SS-ANOVA) for the analysis. The bar chart in Fig. 12 depicts the effect of independent variables or combined parameters effect on the objectives. As seen, the NOx emission is mostly influenced by the start of combustion with 0.852 contribution index followed by H2 injection. Regarding entropy and work outputs, the compressor pressure ratio of the turbocharger element is a key factor. The combustion timing influences the thermal gradient in the chamber and greatly impacts the NOx pathway and production. The H2 compression and injection define the entropy variation, which indicates the exergy destruction and irrevesibility.

The hydrogen combustion in engine setting is critical and challenging in terms of achieving a sustainable fuel burning. From industrial perspective, the hydrogen operated engines can provide an environmentally friendly power and electricity generation along with the discussions for circular green economy. The result of this study paves the way for smart hydrogen engine function with instant and online input variable control for minimal entropy generation and NOx production of hydrogen engine while keeping the output work in a maximum level. The outcome of this investigation provides an overarching framework for a sustainable cold-ironing and transportation clusters especially in automotive and maritime sectors. A similar study is compared with this work from different aspects listed in Table 6.

## 5. Conclusion

A turbocharged propulsion system is designed 1-dimensionally to be powered with dual-fuel diesel-hydrogen. This power system must be upgraded based on the efficiency of power output while keeping the NO emission below a specified threshold and minimising the irreversibilities by lowering the entropy generation. The 1D gas dynamic modeling is coupled to the optimiser interface and two methods of optimisation are tested (evolutionary and heuristic) with different DoE sampling strategies. The multi-objective function is formulated with two different weighting to NO emission, entropy, and volume work by adjusting the operational inputs of H2 mass injection, turbocharger efficiency, air compression ratio, and start of combustion. The following is the gist of key findings in this study.

1 For MOGT and NSGA-II different input parameters effect size and effect direction can be identified. While Rp is the dominant factor influencing the entropy with NSGA-II, the H2 injection is the most influential parameter on entropy with MOGT. However, for NO emission both optimisers show that SoC is the most significant factor with 54.3% and 45.6% share for NSGA-II and MOGT, respectively. On the other hand, H2 injection has the direct impact on volume work based on NSGA-II whereas it causes an inverse impact on the volume work.

2 MOGT is faster than NSGA-II in finding the best solution; game theory optimizer explores and finds the best solution at ID92 where genetic algorithm is able to introduce its best case at ID95. The objective function value for MOGT is 2.49 which is greater than the objective function value of NSGA-II corresponding to 2.36.

3 By implementing the optimisation, the in-cylinder peak pressure and peak work output ratio increases significantly (18.2% and 24.8%) compared to the baseline powertrain configuration (with MOGT), while it is possible to reduce the NO well below the $3.2 \times 10^{-4}$ limit (as constraint) and reduce the entropy generation in an attempt to promote the second law of thermodynamics governing the energy quality of the energy systems.

4 It is noted that although MOGT is more successful in optimising the objective parameters of interest, NSGA-II best case can result in better responses for CO emission and lower fuel consumption.

These findings provide valuable insights for the development of advanced dual-fuel engine control strategies, enabling a balance between performance optimisation and emissions reduction.

## CRediT authorship contribution statement

**Hadi Taghavifar:** Writing – review & editing, Writing – original draft, Visualization, Methodology, Investigation, Conceptualization. **Sumit Roy:** Writing – review & editing, Validation, Methodology, Investigation, Formal analysis. **Anthony Paul Roskilly:** Supervision, Resources, Project administration, Formal analysis.

## Declaration of competing interest

The authors declare that they have no known competing financial interests or personal relationships that could have appeared to influence the work reported in this paper.

## Acknowledgments

This research work was funded by the Engineering and Physical Science Research Council of UK (Grant number: EP/T022949/1).

## References

[1] Cervantes-Bobadilla M, Escobar-Jiménez RF, Gómez-Aguilar JF, García-Morales J, Olivares-Peregrino VH. Experimental study on the performance of controllers for the hydrogen gas production demanded by an internal combustion engine. Energies 2018;11(8):2157.
[2] Wang H, Ji C, Shi C, Ge Y, Meng H, Yang J, Chang K, Yang Z, Wang S, Wang X. Modeling and parametric study of the performance-emissions trade-off of a hydrogen Wankel rotary engine. Fuel 2022;318:123662.
[3] Benajes J, Novella R, Gomez-Soriano J, Barbery I, Libert C. Advantages of hydrogen addition in a passive pre-chamber ignited SI engine for passenger car applications. Int J Energy Res 2021;45(9):13219–37.
[4] Li Y, Gao W, Zhang P, Fu Z, Cao X. Influence of the equivalence ratio on the knock and performance of a hydrogen direct injection internal combustion engine under different compression ratios. Int J Hydrogen Energy 2021;46(21):11982–93.
[5] Oikawa M, Kojiya Y, Sato R, Goma K, Takagi Y, Mihara Y. Effect of supercharging on improving thermal efficiency and modifying combustion characteristics in lean-burn direct-injection near-zero-emission hydrogen engines. Int J Hydrogen Energy 2022;47(2):1319–27.
[6] Sorensen B, Spazzafumo G. Hydrogen and fuel cells: emerging technologies and applications. 2018.
[7] Gupta R, Basile A, Veziroglu TN, editors. Compendium of hydrogen energy: hydrogen storage, distribution and infrastructure. Woodhead Publishing; 2016.
[8] White CM, Steeper RR, Lutz AE. The hydrogen-fueled internal combustion engine: a technical review. Int J Hydrogen Energy 2006;31(10):1292–305.
[9] Taghavifar H, Khalilarya S, Jafarmadar S. Adaptive neuro-fuzzy system (ANFIS) based appraisal of accumulated heat from hydrogen-fueled engine. Int J Hydrogen Energy 2015;40(25):8206–18.
[10] Taghavifar H, Mazari F. 1D diesel engine cycle modeling integrated with MOPSO optimization for improved NOx control and pressure boost. Energy 2022;247:123517.
[11] Teodosio L, Berni F. Optimization via genetic algorithm of a variable-valve-actuation spark-ignition engine based on the integration between 1D/3D simulation codes and optimizer. Int J Engine Res 2023;24(4):1760–84.
[12] Misul DA, Scopelliti A, Baratta M. High-performance hydrogen-fueled internal combustion engines: feasibility study and optimization via 1D-CFD modeling. Energies 2024;17(7):1593.
[13] Veza I, Karaoglan AD, İleri E, Afzal A, Hoang AT, Tamaldin N, Herawan SG, Abbas MM, Said MFM. Multi-objective optimization of diesel engine performance and emission using grasshopper optimization algorithm. Fuel 2022;323:124303.
[14] Silva M, Mohan B, Badra J, Zhang A, Hlaing P, Cenker E, AlRamadan AS, Im HG. DoE-ML guided optimization of an active pre-chamber geometry using CFD. Int J Engine Res 2023;24(7):2936–48.
[15] Castresana J, Gabina G, Martin L, Uriondo Z. Comparative performance and emissions assessments of a single-cylinder diesel engine using artificial neural network and thermodynamic simulation. Appl Therm Eng 2021;185:116343.
[16] Jena P, Tirkey JV. Power and efficiency improvement of SI engine fueled with boosted producer gas-methane blends and LIVC-miller cycle strategy: thermodynamic and optimization studies. Energy 2024;289:130068.
[17] Wang Y, Wang G, Yao G, Shen Q, Yu X, He S. Combining GA-SVM and NSGA-III multi-objective optimization to reduce the emission and fuel consumption of high-pressure common-rail diesel engine. Energy 2023;278:127965.
[18] Taghavifar H, Nemati A, Salvador FJ, De la Morena J. 1D energy, exergy, and performance assessment of turbocharged diesel/hydrogen RCCI engine at different levels of diesel, hydrogen, compressor pressure ratio, and combustion duration. Int J Hydrogen Energy 2021;46(42):22180–94.
[19] Gautam PS, Vishnoi PK, Gupta VK. A single zone thermodynamic simulation model for predicting the combustion and performance characteristics of a CI engine and its validation using statistical analysis. Fuel 2022;315:123285.
[20] Wang Y, He G, Huang H, Guo X, Xing K, Liu S, Tu Z, Xia Q. Thermodynamic and exergy analysis of high compression ratio coupled with late intake valve closing to improve thermal efficiency of two-stage turbocharged diesel engines. Energy 2023;268:126733.
[21] Chaudhary VP, Singh MK, Lata DB. Optimization of performance and emission parameters of hydrogen enriched dual fuel diesel engine using response surface methodology. Int J Hydrogen Energy 2024;79:1100–12.
[22] Khan O, Khan MZ, Bhatt BK, Alam MT, Tripathi M. Multi-objective optimization of diesel engine performance, vibration and emission parameters employing blends of biodiesel, hydrogen and cerium oxide nanoparticles with the aid of response surface methodology approach. Int J Hydrogen Energy 2023;48(56):21513–29.
[23] Lawrence KR, Anchupogu P, Reddygari MR, Gangula VR, Balasubramanian D, Veerasamy S. Optimization of biodiesel yield and performance investigations on diesel engine powered with hydrogen and acetylene gas injected with enriched Jojoba biodiesel blend. Int J Hydrogen Energy 2024;50:502–23.
[24] Bae J, Ju K, Kim J, Park J. Numerical investigation and Pareto optimization on performance, emission and in-cylinder reforming characteristics for two cylinder reciprocating engine with COx free fuel. Int J Hydrogen Energy 2023;48(27):10272–87.
[25] Boost Avl. Users guide for AVL BOOST – AVL list GmbH. 2021.
[26] Noske G. Ein quasidimensionales Modell zur Beschreibung des ottomotorischen Verbrennungsablaufes. VDI-Verlag; 1988.
[27] Woschni, G., "A universally applicable equation for the instantaneous heat transfer coefficient in internal combustion engines", SAE 6700931.
[28] Pattas K, Häfner G. Formation of nitrogen oxides in gasoline engine combustion. Engine Technology Z. 1973;34(12).
[29] Taghavifar H, Mazari F. 1D diesel engine cycle modeling integrated with MOPSO optimization for improved NOx control and pressure boost. Energy 2022;247:123517.
[30] ModeFrontier user's manual. ESTECO 2021.
[31] McKay MD, Conover WJ, Beckman RJ. Latin hypercube sampling: a comparison of three methods for selecting values of input variables in the analysis of output from a computer code. Technometrics 1979;21(2):239–45.
[32] Clarich A, Rigoni E, Poloni C. A new algorithm based on game theory for robust and fast multi-objective optimization. Trieste, Italy: Esteco modeFrontier User Guide; 2003.
[33] Kreps DM. Nash equilibrium. In: Game theory. London: Palgrave Macmillan UK; 1989. p. 167–77.
[34] Fateh N, Parashar S, Silvestri J. *Game theory approach to engine performance optimization* (No. 2008-01-0871). SAE Technical Paper. 2008.
[35] Deb K. A fast elitist non-dominated sorting genetic algorithm for mulit-objedtive optimization: NSGA-II. *KanGAL report 200001*. 2000.
[36] Turco A, Kavka C. MFGA: a GA for complex real-world optimisation problems. Int J Innovat Comput Appl 2011;3(1):31–41.
[37] Salek F, Babaie M, Hosseini SV, Bég OA. Multi-objective optimization of the engine performance and emissions for a hydrogen/gasoline dual-fuel engine equipped with the port water injection system. Int J Hydrogen Energy 2021;46(17):10535–47.